AJNR

Apparent Diffusion Coefficients for Differentiation of Cerebellar Tumors in Children

Z. Rumboldt, D.L.A. Camacho, D. Lake, C.T. Welsh and M. Castillo

AJNR Am J Neuroradiol 2006, 27 (6) 1362-1369
http://www.ajnr.org/content/27/6/1362

ORIGINAL RESEARCH

Apparent Diffusion Coefficients for Differentiation of Cerebellar Tumors in Children

Z. Rumboldt
D.L.A. Camacho
D. Lake
C.T. Welsh
M. Castillo

BACKGROUND AND PURPOSE: Diffusion-weighted imaging (DWI) and apparent diffusion coefficient (ADC) maps provide information at MR imaging that may reflect cell attenuation and integrity. We hypothesized that cerebellar tumors in children can be differentiated by their ADC values.

METHODS: Brain MR imaging studies that included ADC maps were retrospectively reviewed in 32 patients with histologically proved cerebellar neoplasm. There were 17 juvenile pilocytic astrocytomas (JPA), 8 medulloblastomas, 5 ependymomas, and 2 rhabdoid (atypical teratoid/rhabdoid tumor [AT/RT]) tumors. Absolute ADC values of contrast-enhancing solid tumor regions and ADC ratios (ADC of solid tumor to ADC of normal-appearing white matter) were compared with the histologic diagnosis. ADC values and ratios of JPAs, medulloblastomas, and ependymomas were compared by using a 2-tailed *t* test and one-way analysis of variance (ANOVA).

RESULTS: ADC values were significantly higher in pilocytic astrocytomas (1.65 ± 0.27) (mean ± SD) than in ependymomas (1.10 ± 0.11) ($P = .0003$) and medulloblastomas (0.66 ± 0.15) ($P < .0001$). Ependymomas demonstrated significantly higher ADC values than medulloblastomas ($P = .0005$). The observed differences were statistically significant on ANOVA ($P < .001$). ADC ratios were also significantly different among these 3 tumor types. AT/RT ADC values were similar to medulloblastoma. The range of ADC values and ratios within JPAs and ependymomas did not overlap with that of medulloblastomas.

CONCLUSION: Assessment of ADC values of enhancing solid tumor is a simple and reliable technique for preoperative differentiation of cerebellar tumors in pediatric patients. Our cutoff values of $>1.4 \times 10^3$ mm^2/s for JPA and $<0.9 \times 10^3$ mm^2/s for medulloblastoma were 100% specific.

Although MR imaging is essential for diagnosis and evaluation of brain tumors, it offers limited information regarding tumor type and grade and is frequently far from being a definite diagnostic test, which is a role reserved for histology. Accurate preoperative diagnosis is an important goal in pediatric patients with cerebellar neoplasms, because the most common tumors in this location and age group, juvenile pilocytic astrocytoma (JPA) and medulloblastoma, may dictate the need for different surgical approaches and have significantly different natural histories and outcomes.[1]

Diffusion MR imaging is a technique in which dedicated phase-defocusing and -refocusing gradients allow evaluation of microscopic water diffusion within tissues, where calculated apparent diffusion coefficient (ADC) maps represent an absolute measure of average diffusion for each voxel.[2] Diffusion-weighted imaging (DWI) and ADC maps are useful in evaluation of acute infarcts and a number of different brain lesions.[2-5] ADC values in brain tumors seem to be primarily based on tumor cellularity and nuclear area,[6-9] and a correlation between ADC values and tumor grade also seems to be present, though the reported studies have demonstrated conflicting results.[5-16] Significant differences in cellularity of pediatric cerebellar neoplasms, particularly between JPAs and medulloblastomas, indicate that these lesions could potentially be distinguished by their ADC values.[8,17]

The goal of our retrospective study was to establish the ADC values of different pediatric cerebellar tumors with the hypothesis that these ADC values and ratios allow for differentiation of specific tumor types.

Received July 26, 2005; accepted after revision October 17.

From the Departments of Radiology (Z.R., D.L.) and Pathology and Laboratory Medicine (C.T.W.), Medical University of South Carolina, Charleston, SC; and Department of Radiology (D.L.A.C., M.C.), University of North Carolina, Chapel Hill, NC.

Address correspondence to Zoran Rumboldt, MD, Department of Radiology, Medical University of South Carolina, 169 Ashley Ave, P.O. Box 250322, Charleston, SC 29425.

Methods

Retrospective review of patient records with histologically proved neoplasm in an electronic data base and PACS was performed in 2 institutions. Histologic diagnosis and MR imaging studies were evaluated for all pediatric patients with cerebellar neoplasm. Histologic diagnosis was provided by analysis of postoperative specimens.

Thirty-two patients in whom ADC maps were obtained in addition to conventional MR imaging were identified and included in the study. There were 18 male patients and 16 female patients, with a mean age of 9 years (range, 6 weeks to 23 years). Histologic examination revealed 17 (53.1%) patients with JPA, 8 (25%) with medulloblastoma, 5 (15.6%) with ependymoma, and 2 (6.3%) with rhabdoid tumor (atypical teratoid/rhabdoid tumor [AT/RT]). In all but 2 patients, the initial presentation MR imaging study was used for analysis; in these 2 patients, postoperative MR imaging showing residual tumor was used.

Conventional MR imaging was performed on 1.5T MR units with a protocol that included sagittal noncontrast T1-weighted, axial fast spin-echo T2-weighted, axial fluid-attenuated inversion recovery (FLAIR), as well as postcontrast enhanced axial, coronal, and sagittal T1-weighted images. Diffusion-weighted images were acquired (before administration of contrast material) by using b values of 0, 500, and 1000 s/mm^2 applied in the *Z*, *Y*, and *X* directions. Processing of ADC maps was performed automatically on the MR scanners.

For each patient the enhancing solid portion of the lesion was identified on postcontrast T1-weighted images and matching ADC maps. Regions of interest (ROIs) of 50–100 mm^2 were accordingly manually positioned at the PACS workstations (AGFA Impax 4.1, Mortsel, Belgium) and all values were automatically calculated and expressed in 10^{-3} mm^2/s. The persons placing the ROIs were blinded

Table 1. Data and ratios of apparent diffusion coefficient (ADC) values with 1-ROI and 3-ROI methods

Patient No. Age/Sex	Tumor Histology	ADC Tumor	ADC Tumor Average	Ratio 1-ROI method	Ratio 3-ROI method
1/14 y/M	JPA	1.45	1.44	2.02	1.93
2/7 y/M	JPA	1.28	1.24	1.76	1.65
3/20 mo/M	JPA	1.64	1.66	2.18	1.90
4/11 y/M	JPA	1.44	1.45	2.02	1.97
5/15 y/M	JPA	1.65	1.83	2.43	2.48
6/15 y/F	JPA	2.01	1.97	2.93	2.70
7/6 y/F	JPA	1.39	1.29	1.94	1.67
8/6 y/M	JPA	1.89	1.86	2.72	2.50
9/3 y/M	JPA	1.44	1.48	1.62	1.77
10/21 y/M	JPA	1.38	1.43	1.66	1.70
11/4 y/F	JPA	1.60	1.85	2.47	2.50
12/7 y/M	JPA	1.62	1.60	1.84	1.90
13/6 y/M	JPA	1.73	1.74	2.01	2.12
14/4 y/F	JPA	1.54	1.58	2.26	2.16
15/15 y/F	JPA	2.09	1.93	2.99	2.76
16/7 y/M	JPA	1.49	1.46	1.84	1.87
17/2 y/F	JPA	2.05	2.11	2.30	2.21
18/8 y/M	Ependymoma	1.08	0.97	1.28	1.15
19/16 y/M	Ependymoma	1.11	1.05	1.39	1.31
20/4 y/F	Ependymoma	1.24	1.15	1.39	1.44
21/5 y/F	Ependymoma	1.07	1.05	1.43	1.42
22/22 y/F	Ependymoma	1.29	1.26	1.85	1.63
23/16 y/M	Medulloblastoma	0.69	0.68	1.00	0.91
24/3 y/M	Medulloblastoma	0.90	0.93	1.07	1.10
25/22 y/F	Medulloblastoma	0.48	0.49	0.71	0.71
26/23 y/F	Medulloblastoma	0.54	0.48	0.71	0.66
27/7 y/F	Medulloblastoma	0.74	0.69	1.02	0.91
28/11 y/M	Medulloblastoma	0.61	0.57	0.77	0.74
29/2 y/F	Medulloblastoma	0.58	0.60	0.79	0.82
30/6 wk/M	Medulloblastoma	0.80	0.80	0.84	0.84
31/13 mo/F	AT/RT	0.60	0.63	0.69	0.74
32/15 mo/M	AT/RT	0.55	0.56	0.69	0.64

Note:—1-ROI method indicates the approach wherein a single region of interest of solid enhancing tumor to normal-appearing cerebellum was performed; 3-ROI method, approach used by placing additional regions of interest in the tumor and bilateral centrum semiovale.
ADC values are expressed in 10^{-3} mm^2/s. JPA indicates juvenile pilocytic astrocytoma; AT/RT, atypical teratoid/rhabdoid tumor.

to the tumor histology. The first region of interest was placed over homogenous enhancing regions in the central portion of tumors. Two additional ROIs were placed on homogenous enhancing areas on different sections, or, if the tumor was present on fewer than 3 sections, these ROIs were positioned so that overlapping with the first ROI was avoided. A total of 3 lesion ROIs were obtained and averaged to serve as the ADC tumor average value. Control ADC values were obtained by placing ROIs in the normal-appearing cerebellum, as well as bilateral centrum semiovale (3-region-of-interest method). The control ADC values in the normal brain were compared among patients with different tumors. The ADC values of each tumor type were compared with their respective control ADC values. The ratio of the average tumor ADC to the average control ADC of the normal-appearing cerebellum, contralateral and ipsilateral supratentorial brain ROI was then computed (ADC ratio). In addition, the ratio of a single ROI (the first measurement) of solid enhancing tumor to normal-appearing cerebellum was also performed (1-region-of-interest method) to determine whether the 3-region-of-interest and 1-region-of-interest methods yielded similar results.

Comparison of obtained normal brain and tumor ADC values was done by using a 2-tailed paired *t* test, whereas comparison of ADC values and ratios among groups was performed with a 2-tailed unpaired *t* test. One-way analysis of variance (ANOVA) was also performed, including the Tukey honestly significant difference test and the Duncan method for pairwise multiple comparison procedures. The observed differences were considered statistically significant if P was less than .05. Because of the small number, the AT/RT tumor group was excluded from statistical analysis.

After obtaining the above information, a first-year radiology resident, who was informed that JPAs should be bright and medulloblastomas dark, reviewed isolated ADC maps belonging to all patients with these 2 tumors and tried to correctly identify them based on this single criterion. The obtained sensitivity, specificity, and accuracy were calculated.

Results

The results are summarized in Tables 1 and 2 and in Fig 1. Normal brain ADC values among patients with JPAs, medulloblastomas, and ependymomas were not significantly different ($P = .75$–$.87$). There was no significant difference in all ADC tumor values obtained with 3-region-of-interest compared with 1-region-of-interest methods ($P = .524$). In patients with JPA, the average normal brain versus tumor ADC value was significantly different ($P < .0001$). In patients with medulloblastoma and ependymoma, this difference was also statistically significant ($P = .015$ and $P = .0066$, respectively).

JPA and medulloblastoma could be differentiated by using both absolute values and ratios (Table 2, Figs 1–5). The JPA group showed significantly higher ADC values based on 3 measurements ($P < .0001$) and with the single measurement

Table 2. Summary of apparent diffusion coefficient (ADC) values of tumors, ADC ratios of tumors to normal-appearing brain, and ADC values of normal-appearing brain parenchyma for juvenile pilocytic astrocytomas (JPA), ependymomas, and medulloblastomas

	JPA	Ependymoma	Medulloblastoma
Tumor ADC range (1-ROI and 3-ROI) ($\times 10^{-3}$ mm^2/s)	1.24–2.09	0.97–1.29	0.48–0.93
Mean tumor ADC value (3-ROI) ($\times 10^{-3}$ mm^2/s) ($\pm$SD)	1.65 $\pm$ 0.27	1.10 $\pm$ 0.11	0.66 $\pm$ 0.15
Tumor ADC ratio range (1-ROI and 3-ROI)	1.62–2.99	1.15–1.85	0.66–1.10
Mean tumor ADC ratio (3-ROI) ($\pm$SD)	2.11 $\pm$ 0.36	1.39 $\pm$ 0.18	0.84 $\pm$ 0.14
Mean tumor ADC ratio (1-ROI) ($\pm$SD)	2.18 $\pm$ 0.42	1.47 $\pm$ 0.22	0.86 $\pm$ 0.15
Normal brain ADC (3-ROI) ($\pm$SD)	0.78 $\pm$ 0.07	0.79 $\pm$ 0.04	0.78 $\pm$ 0.08
Age range (Mean Age)	20 mo–21 y (8.5 y)	4 y–22 y (11 y)	6 wk–23 y (10.5 y)

Note:—1-ROI method indicates the approach wherein a single region of interest of solid enhancing tumor to normal-appearing cerebellum was performed; 3-ROI method, approach used by placing additional regions of interest in the tumor and bilateral centrum semiovale.

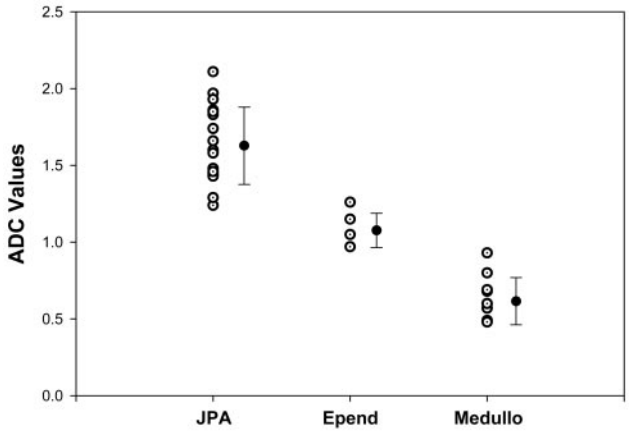

Fig 1. Scatter diagram of average ADC tumor values for all pilocytic astrocytomas (JPA), ependymomas (Epend) and medulloblastomas (Medullo) (open circles) along with their respective mean (full circles) and standard deviation (bars) values. ADC values are expressed in 10^{-3} mm^2/s.

technique ($P < .0001$), as well as significantly higher ADC ratio values with both the 3-region-of-interest ($P < .0001$) and 1-region-of-interest ($P < .0001$) techniques. There was no overlap in individual tumor ADC values or ratios between JPA and medulloblastoma or AT/RT (Tables 1 and 2 and Fig 1). JPA also demonstrated higher diffusion compared with ependymoma (Table 2 and Figs 1, 2, 4 and 7) and the observed difference was statistically significant for 3-region-of-interest ($P = .0002$) and 1-region-of-interest ($P = .0006$) ADC measurements, as well as for ADC ratios obtained with 3-region-of-interest ($P = .0004$) or 1-region-of-interest ($P = .018$) techniques.

The ADC values of ependymoma were higher than of medulloblastoma (Table 2, Figs 1, 3, 5, and 7), and this was statistically significant for both 3-region-of-interest ($P = .0002$) and 1-region-of-interest ($P < .0001$) measurements, as well as for 3-region-of-interest ($P < .0001$) and 1-region-of-interest ($P = .0001$) ADC ratio techniques. There was no overlap in individual tumor ADC values or ratios between ependymoma and medulloblastoma or AT/RT (Tables 1 and 2 and Fig 1). The values obtained for AT/RT were within the range of medulloblastoma group with any of the performed measurements (Table 1, Figs 3, 5, and 6).

Source of variation between groups of average tumor ADC values for JPA, medulloblastoma, and ependymoma was also statistically significant with one-way ANOVA at $P < .001$ level. Pairwise comparison between any of these groups was also statistically significant at $P < .01$ level with the Tukey honestly significant difference test and at $P < .05$ with the Duncan method.

On subjective evaluation of the images, JPAs were very hyperintense, ependymomas were isointense to slightly hyperintense, and medulloblastomas and AT/RTs predominantly hypointense compared with brain parenchyma on ADC maps (Figs 2–7). The first-year radiology resident evaluating isolated ADC maps of 17 JPAs and 8 medulloblastomas was able to correctly identify the tumor type in all cases, yielding sensitivity, specificity, and accuracy of 100%.

Discussion

MR diffusion imaging has been widely used to study cerebral infarction, multiple sclerosis, tumors, abscesses, and other intracranial diseases and has become an indispensable part of many brain MR imaging protocols, for adult and pediatric patients alike.[18] It is a reliable technique for detection of acute infarcts, as well as for distinction between arachnoid cysts and epidermoids, and between brain tumors and abscesses.[2-16] Arachnoid cysts demonstrate free diffusion of water similar to that of CSF, whereas epidermoids show slower diffusion, presumably as a result of the more complex internal structure.[3,4] The ADC values of abscess fluid are markedly lower than those of necrotic or cystic portions of tumor, which is considered to be a consequence of restricted water mobility within purulent fluid related to its high cellularity and viscosity.[3,4] Diffusion MR imaging is also helpful for distinguishing primary central nervous system lymphoma and toxoplasmosis in patients infected with human immunodeficiency virus.[19]

Although a negative correlation between glioma grade and ADC values has been established,[11,14,16,17] generalized application of ADC values for differentiation of brain tumor types and grades has been found inaccurate.[7] ADC also does not seem helpful in distinguishing tumor tissue from peritumoral edema.[20] On the other hand, the ADC has been reported reliable for distinction of specific tumor types, such as dysembryoplastic neuroepithelial tumors,[15] and helpful in characterizing some pediatric brain tumors.[8,21] In addition, pretreatment diffusion values also seem to be predictive of tumor response to radiation therapy[22] and valuable for differentiation of radiation-induced brain injury from tumor recurrence.[23,24]

None of the prior reports specifically evaluated ADC values of cerebellar tumors in pediatric population—the studies included all intracranial tumors, and only one of them was limited to children.[8] Either the values for all primitive neuroectodermal tumors (PNETs), JPAs, and ependymomas arising in

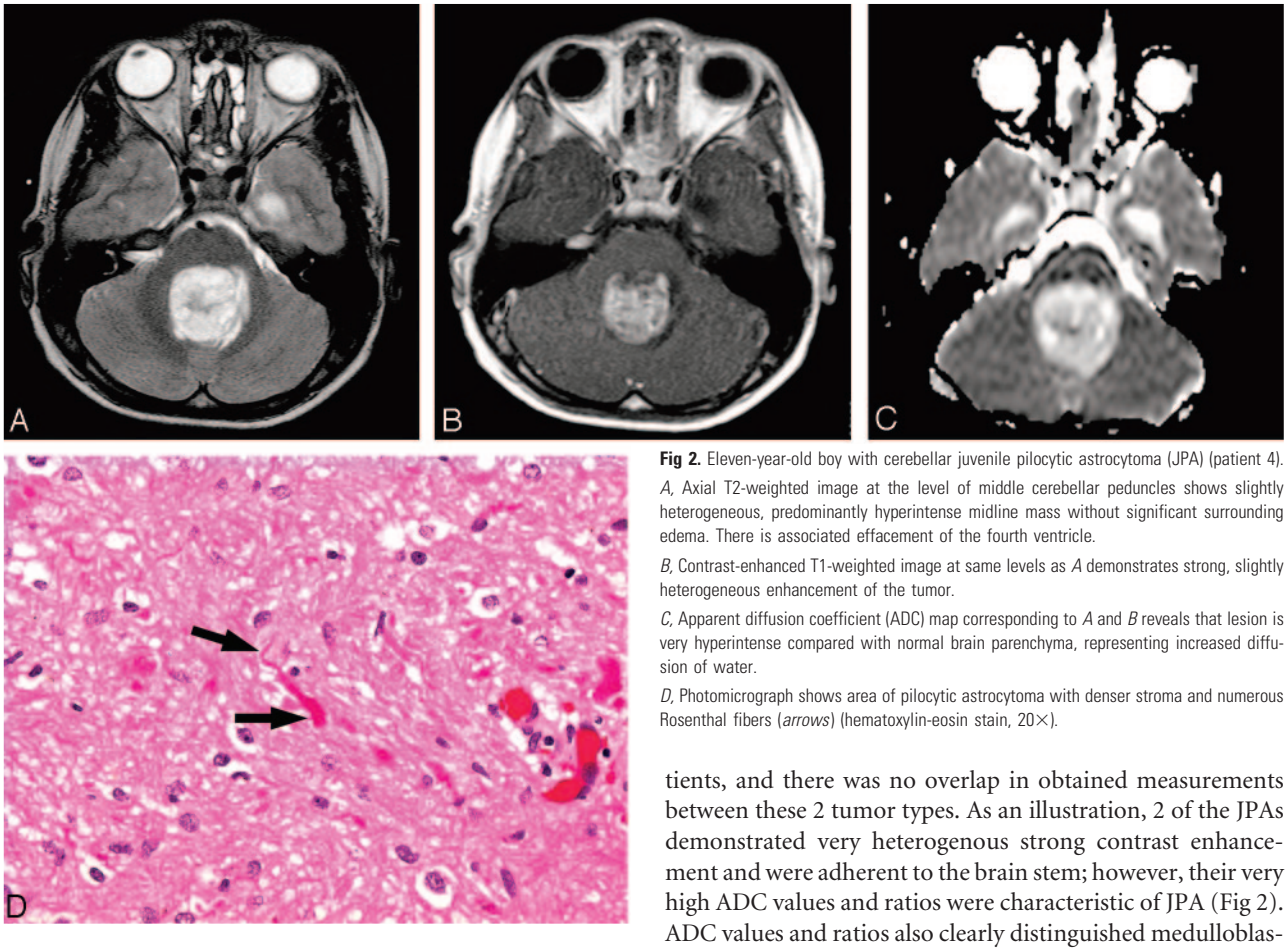

Fig 2. Eleven-year-old boy with cerebellar juvenile pilocytic astrocytoma (JPA) (patient 4).

A, Axial T2-weighted image at the level of middle cerebellar peduncles shows slightly heterogeneous, predominantly hyperintense midline mass without significant surrounding edema. There is associated effacement of the fourth ventricle.

B, Contrast-enhanced T1-weighted image at same levels as *A* demonstrates strong, slightly heterogeneous enhancement of the tumor.

C, Apparent diffusion coefficient (ADC) map corresponding to *A* and *B* reveals that lesion is very hyperintense compared with normal brain parenchyma, representing increased diffusion of water.

D, Photomicrograph shows area of pilocytic astrocytoma with denser stroma and numerous Rosenthal fibers (*arrows*) (hematoxylin-eosin stain, 20×).

any intracranial location and in any age group were combined together,[15] or the goal of the study was to investigate possible correlation between cellular attenuation and nuclear area with ADC values.[8] Direct comparison of different histologic types of pediatric cerebellar tumors has not yet been performed.

The ADC values of different tumor types obtained in our study are comparable with those reported in the literature[8,15] (Table 3). At least some of the discrepancies in the ADC values among the studies are probably due to different designs: Yamasaki et al[15] included patients of all age groups, whereas both Gauvain et al[8] and Yamasaki et al[15] evaluated all intracranial tumors, infratentorial and supratentorial (Table 3).

It has been established that ADC values of normal developing brain decrease with increasing age.[25-27] The absolute ADC value, rather than ADC ratio, may therefore be the preferred method of differentiating pediatric brain tumors because diffusion properties of brain change with age, in addition to white matter anisotropy and partial volume averaging effects, which also affect the ADC ratio measurements. However, ADC ratios have been used in previously reported studies,[2-24] and we wanted to test these ratios because they correspond to qualitative estimate of relative tumor intensity on visual inspection. If the tumor type could be determined based on qualitative subjective evaluation of ADC maps, without measurements, the method would be more practical and easier to implement in clinical practice.

In our study, JPA and medulloblastoma could be differentiated on the basis of ADC values and ADC ratios in all patients, and there was no overlap in obtained measurements between these 2 tumor types. As an illustration, 2 of the JPAs demonstrated very heterogenous strong contrast enhancement and were adherent to the brain stem; however, their very high ADC values and ratios were characteristic of JPA (Fig 2). ADC values and ratios also clearly distinguished medulloblastoma from ependymoma in all patients, again without any overlap. This finding is similar to that in a recent study by Yamasaki et al[15] who found that ADC values were retrospectively 100% accurate in differentiation between ependymomas and PNETs.

The ADC values of JPAs were also higher from ependymomas in our study, and this difference was statistically significant ($P = .0002$ and $P = .0006$, for 1-region-of-interest and 3-region-of-interest methods, respectively), though there was a slight overlap in measurements, which corresponds to results reported by Yamasaki et al.[15] Medulloblastomas and AT/RTs may be indistinguishable by their diffusion characteristics on MR imaging.

These findings in JPAs and medulloblastomas are probably secondary to the low cellularity and relatively small nuclear area typically seen in the former tumor types in contradistinction to the densely packed cells and large nuclei characteristic for the latter.[8,28-30] Kotsenas et al[17] described a case of a medulloblastoma that was very hyperintense on DWI and theorized that the attenuated cellularity of the tumor resulted in this increased signal intensity and was due to relatively restricted diffusion. A number of studies have since reported that increasing cellularity leads to increased signal intensity on DWI and consequently hypointensity on ADC maps.[6-9,13]

The high cellularity of medulloblastoma is a well-known histologic feature of these tumors.[28,29] Medulloblastoma characteristically shows patternless sheets of small cells with small areas of necrosis. The cells, though small, actually vary in size and shape (Fig 3*D*). Histologic variants of medulloblastoma

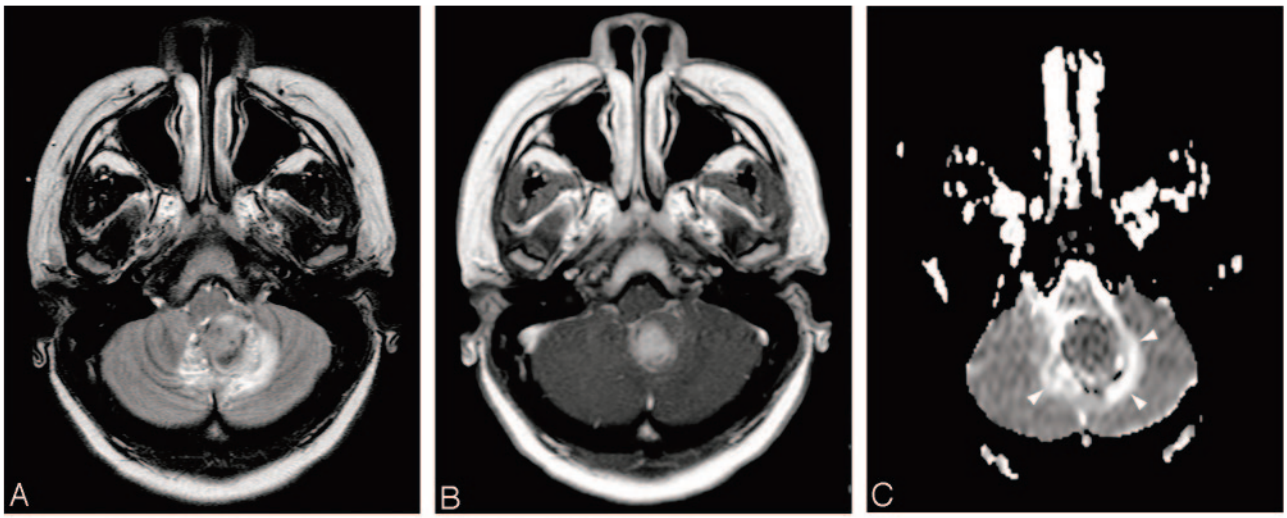

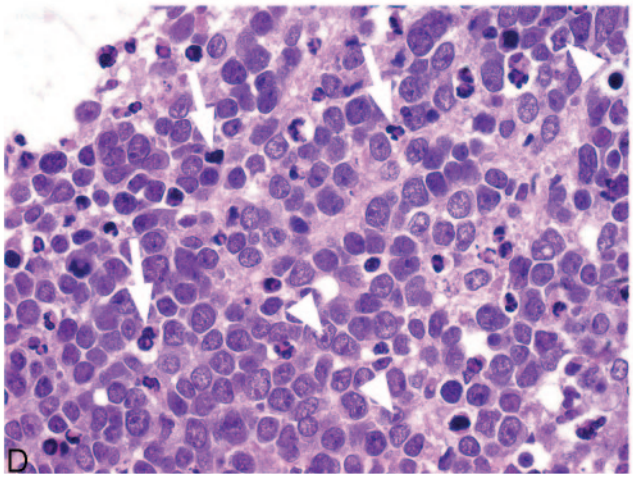

Fig 3. Sixteen-year-old boy with cerebellar medulloblastoma (patient 23).

A, Axial T2-weighted image at level of medulla oblongata shows heterogeneous mass in left paramedian location that is predominantly hyperintense. There is surrounding edema and compression of fourth ventricle.

B, Contrast-enhanced T1-weighted image corresponding to *A* demonstrates avid, slightly heterogeneous, enhancement of tumor.

C, ADC map corresponding to *A* and *B* reveals that mass is hypointense to normal cerebellar parenchyma, consistent with decreased diffusion. Hyperintense ring surrounding tumor (*arrowhead*) represents increased diffusion of vasogenic edema.

D, Photomicrograph shows densely packed nuclei in medulloblastoma with scattered apoptosis and mitoses (*arrows*). Some nuclei show prominent nucleoli (*arrowheads*) (hematoxylin-eosin stain, 40×).

include the nodular/desmoplastic pattern, a large cell/anaplastic category, and tumors with additional differentiation (neuronal, glial, striated muscle, or melanin-producing cells). Desmoplastic/nodular medulloblastomas have prominent nodules that are paler than the surrounding tumor on histologic sections due to more stroma and fewer nuclei. These areas, however, remain more densely cellular than the most cellular areas in a typical pilocytic tumor. In one of our patients (patient 25), histologic examination revealed a desmoplastic subtype of medulloblastoma (Fig 5), which was not different from those with the large-cell subtype by conventional MR imaging or ADC values. Although medulloblastomas are typically of low signal intensity on T2-weighted images, in some of our patients, they were predominantly T2 hyperintense and yet they could easily be recognized by ADC values and ratios (Fig 3).

AT/RT tumors have a population of rhabdoid cells and

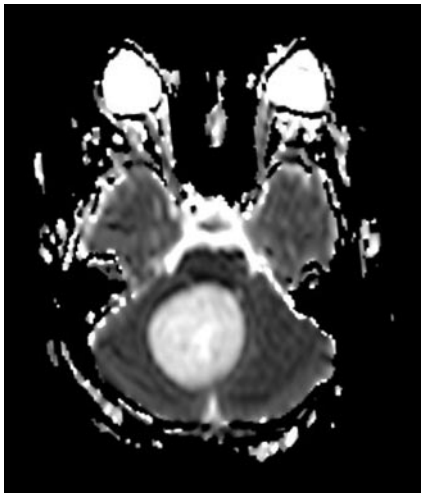

Fig 4. Fifteen-year-old girl with cerebellar JPA (patient 5). ADC map in axial plane at level of middle cerebellar peduncles shows well defined, oval mass in right paramedian location with increased diffusion.

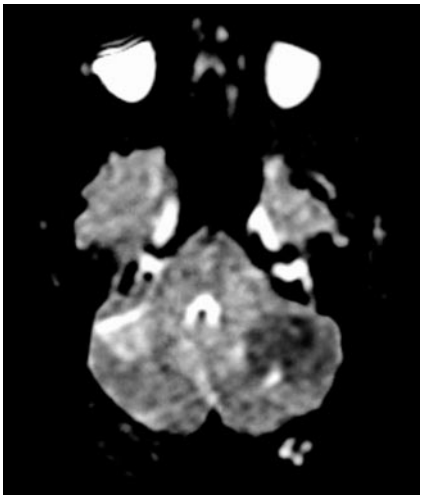

Fig 5. 22-year-old woman with desmoplastic cerebellar medulloblastoma (patient 25). Axial ADC map at level of middle cerebellar peduncles reveals lesion of decreased diffusion in left cerebellar hemisphere. No significant surrounding edema is seen.

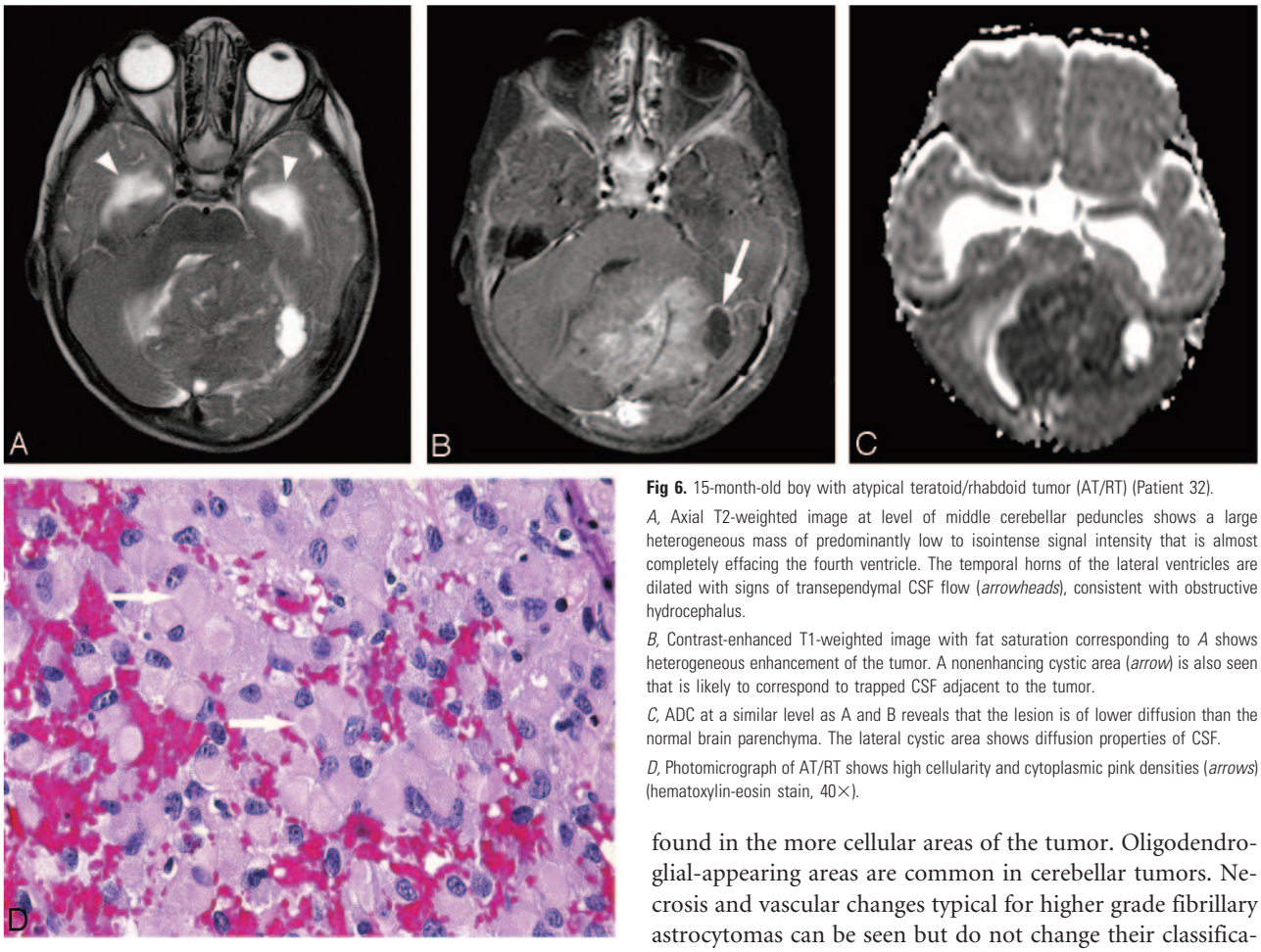

Fig 6. 15-month-old boy with atypical teratoid/rhabdoid tumor (AT/RT) (Patient 32).

A, Axial T2-weighted image at level of middle cerebellar peduncles shows a large heterogeneous mass of predominantly low to isointense signal intensity that is almost completely effacing the fourth ventricle. The temporal horns of the lateral ventricles are dilated with signs of transependymal CSF flow (*arrowheads*), consistent with obstructive hydrocephalus.

B, Contrast-enhanced T1-weighted image with fat saturation corresponding to *A* shows heterogeneous enhancement of the tumor. A nonenhancing cystic area (*arrow*) is also seen that is likely to correspond to trapped CSF adjacent to the tumor.

C, ADC at a similar level as A and B reveals that the lesion is of lower diffusion than the normal brain parenchyma. The lateral cystic area shows diffusion properties of CSF.

D, Photomicrograph of AT/RT shows high cellularity and cytoplasmic pink densities (*arrows*) (hematoxylin-eosin stain, 40×).

often additional variable amounts of other elements, such as neuroectodermal, epithelial, or mesenchymal histology. Rhabdoid cells have an eccentric round-to-oval nucleus with cytoplasmic eosinophilia that varies from granular to characteristic dense pink bodies (Fig 6*D*). The cells may vary in size from small to enormous. Hemorrhage and necrosis are common; mitoses are abundant. On ultrastructural studies, the dense pink inclusions are whorled bundles of intermediate filaments.[29] The tumors are always quite cellular, on the order of the other neoplasm most often in the differential diagnosis (ie, medulloblastoma). Intracranially, these rare tumors usually occur in the cerebellum and are typically of heterogenous appearance on MR imaging.[30] ADC value of AT/RT tumor has been previously reported in only 1 case,[8] and was very similar to the 2 cases in our study (Table 3).

Low water diffusion observed in pilocytic astrocytomas probably reflects the low cellularity appearance of these tumors on histologic examination.[29,31] Pilocytic astrocytomas in the posterior fossa have a classic "biphasic pattern," with alternating loose (vacuolated) and denser areas. Even the denser areas, however, are not particularly cellular, especially compared with medulloblastoma. In pilocytic astrocytomas, there are frequently microcysts in addition to the macrocysts seen on imaging studies (Fig 2*D*). The "piloid" cells for which the tumor is named have oval nuclei and long bipolar processes. Rosenthal fibers (Fig 2*D*), though not pathognomonic of pilocytic astrocytoma, are characteristic. They are generally found in the more cellular areas of the tumor. Oligodendroglial-appearing areas are common in cerebellar tumors. Necrosis and vascular changes typical for higher grade fibrillary astrocytomas can be seen but do not change their classification, grade, or prognosis.

Ependymomas are well circumscribed, moderately cellular tumors. The typical cellularity in posterior fossa ependymomas therefore is somewhere between that of astrocytomas and medulloblastomas. The characteristic histology shows perivascular pseudorosettes (cleared areas and radially arranged cells around blood vessels) (Fig 7*D*) and occasionally ependymal rosettes (cleared spaces and radially arranged cells around a lumen that is not vascular). Several variants exist that are uncommon, one of which is more cellular. As ependymomas progress in malignancy, they also increase in cellularity, but anaplastic ependymomas are also less common than the more benign variants.[29]

Gauvain et al[8] used diffusion tensor imaging, which requires additional postprocessing steps, to examine pediatric tumor cellularity and nuclear-to-cytoplasmic ratio and found that it may be predictive of tumor classification and may enhance the diagnostic process of pediatric brain malignancies. Moreno-Torres et al[32] recently used taurine detection by single-voxel proton MR spectroscopy. In all 6 patients with medulloblastoma, they demonstrated prominent taurine peaks that were absent in the other 7 patients with cerebellar astrocytoma. Although this demonstrates accuracy similar to that of our method, it again involves additional imaging and postprocessing. In our study, we sought to focus on pediatric cerebellar tumors and simplify the evaluation. Our method of analysis can be performed on routinely obtained ADC maps at a PACS station with only a single ROI measurement, without any additional imaging or postprocessing. Our goal of simple

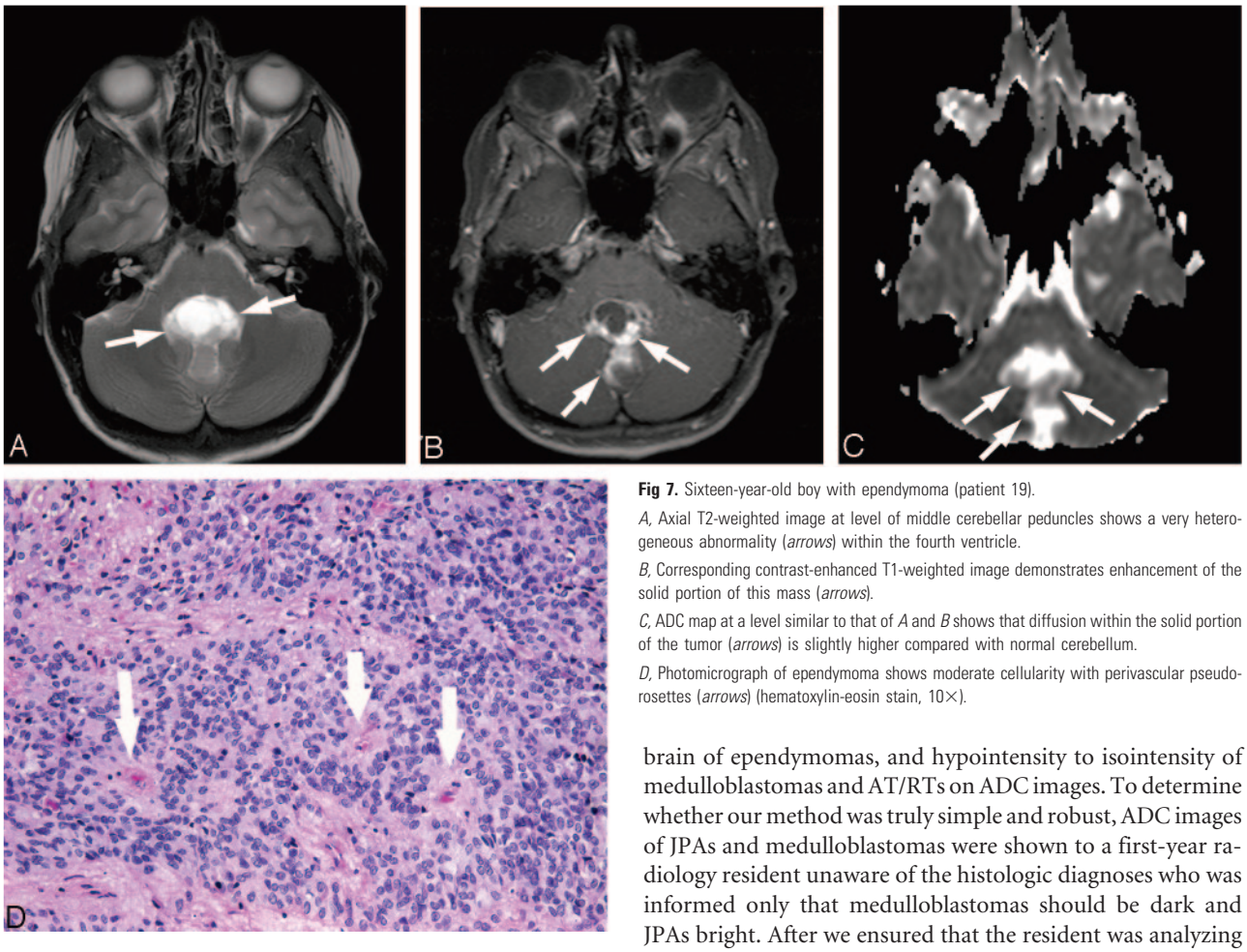

Fig 7. Sixteen-year-old boy with ependymoma (patient 19).

A, Axial T2-weighted image at level of middle cerebellar peduncles shows a very heterogeneous abnormality (*arrows*) within the fourth ventricle.

B, Corresponding contrast-enhanced T1-weighted image demonstrates enhancement of the solid portion of this mass (*arrows*).

C, ADC map at a level similar to that of *A* and *B* shows that diffusion within the solid portion of the tumor (*arrows*) is slightly higher compared with normal cerebellum.

D, Photomicrograph of ependymoma shows moderate cellularity with perivascular pseudorosettes (*arrows*) (hematoxylin-eosin stain, 10×).

Table 3. Summary of apparent diffusion coefficient (ADC) values obtained in 3 studies that evaluated pilocytic astrocytoma (PA), ependymoma, medulloblastoma, and atypical teratoid rhabdoid tumor (AT/RT)

Range of tumor ADC values ($\times 10^{-3}$ mm^2/s)	Gauvain et al 2001[8]	Yamsaki et al 2005[15]*	Present Study
PA	1.13–1.54†	1.30–1.92†	1.24–2.09
Ependymoma	0	1.05–1.33	0.97–1.29
Medulloblastoma	0.54–0.58	0.68–0.99‡	0.48–0.93
AT/RT	0.60§	0	0.55–0.63

*Data for all age groups.
†Data for all intracranial tumors, infratentorial and supratentorial.
‡Data for all intracranial primitive neuroectodermal tumors, including medulloblastoma.
§Data for a supratentorial tumor.

differentiation between the tumors was manifest by comparing the 3-region-of-interest versus the 1-region-of-interest methods. Although the 3-region-of-interest method initially seemed more robust, after careful analysis, the 1-region-of-interest method provided similar results in all patients and further streamlined the analysis.

When ADCs between tumor types were compared for creation of cutoffs, a value of $>1.40 \times 10^{-3}$ mm^2/s was 100% specific for JPA, whereas measurements $<0.90 \times 10^{-3}$ mm^2/s were 100% specific for medulloblastoma and AT/RT. Most of ependymomas fall between 1.00 and 1.30×10^{-3} mm^2/s. On subjective visual inspection, this translates into prominent hyperintensity of JPAs, mild hyperintensity relative to adjacent brain of ependymomas, and hypointensity to isointensity of medulloblastomas and AT/RTs on ADC images. To determine whether our method was truly simple and robust, ADC images of JPAs and medulloblastomas were shown to a first-year radiology resident unaware of the histologic diagnoses who was informed only that medulloblastomas should be dark and JPAs bright. After we ensured that the resident was analyzing the solid enhancing portion of the tumor, he was able to correctly differentiate medulloblastoma from JPA in all patients, indicating that correct distinction of these 2 tumor types is possible by visual inspection only, without additional measurements and even with limited experience.

Limitations of our study include a relatively small number of patients and the limited sample of pathology encountered. A further limitation is the retrospective nature of the analysis. Other less common primary neoplasms occurring in this location were not addressed in our study but deserve further evaluation, particularly in older age groups.

Although ADC values and ratios are not widely reliable in predicting the histology of all brain tumors, we have found that focused application to pediatric patients with posterior fossa tumors is fruitful. ADC values and ratios could prove reliable for distinction of other intracranial tumors, if used in a selective manner to answer specific questions, combined with patient's age, tumor location, and other imaging findings. Isolated analysis of diffusion properties does not provide universally reliable identification of different brain tumor types and grade; however, this may not be clinically relevant, because diagnosis is never based on a single sequence but rather on careful analysis of entire brain MR imaging study. For example, in addition to JPAs, hemangioblastomas and schwannomas are other posterior fossa tumors that have been found to have similar high ADC values.[15,33] These 3 neoplasms may therefore not be distinguished solely on the basis of their diffusion properties; however, extra-axial location of schwanno-

mas and presence of prominent flow voids within hemangioblastomas should allow for correct diagnosis in most cases.

Based on our results, we suggest that ADC values may play a potentially important role in the presurgical management of children with posterior fossa tumors. It may be proposed that if high ADC values are present, a patient may go directly to surgery without additional imaging, given that pilocytic astrocytomas are unlikely to metastasize. Low ADC values on the other hand suggest that the tumor is either a medulloblastoma or a rhabdoid tumor, and imaging of the spine is warranted to exclude metastases and appropriately stage the patient.

Conclusion

ADC values and ratios are simple and readily available techniques for evaluation of pediatric cerebellar neoplasms that may accurately differentiate the 2 most common tumors, JPA and medulloblastoma. Proposed cutoff values of $>1.4 \times 10^{-3}$ mm^2/s for JPA and $<0.9 \times 10^{-3}$ mm^2/s for medulloblastoma seem to reliably provide the diagnosis, which may affect further diagnostic studies, treatment plan, and prognosis. Ependymomas are also significantly different from other tumor types, and in most of cases show ADC values $1.00–1.30 \times 10^{-3}$ mm^2/s.

References

1. Becker L. **Pathology of pediatric brain tumors.** *Neuroimaging Clin N Am* 1999; 9:671–90
2. Rowley HA, Grant PE, Roberts TPL. **Diffusion MR imaging.** *Neuroimaging Clin N Am* 1999;9:343–61
3. Schaefer PW, Grant PE, Gonzalez RG. **Diffusion-weighted MR imaging of the brain.** *Radiology* 2000;217:331–45
4. Castillo M, Mukherji SK. **Diffusion-weighted imaging in the evaluation of intracranial lesions.** *Semin Ultrasound CT MR* 2000;21:405–16
5. Stadnik TW, Chaskis C, Michotte A, et al. **Diffusion-weighted MR imaging of intracerebral masses: comparison with conventional MR imaging and histologic findings.** *AJNR Am J Neuroradiol* 2001;22:969–76
6. Sugahara T, Korogi Y, Kochi M, et al. **Usefulness of diffusion-weighted MRI with echo-planar technique in the evaluation of cellularity of gliomas.** *J Magn Reson Imaging* 1999;9:53–60
7. Gupta RK, Cloughesy TF, Sinha U, et al. **Relationships between choline magnetic resonance spectroscopy, apparent diffusion coefficient and quantitative histopathology in human glioma.** *J Neurooncol* 2000;50:215–26
8. Gauvain KM, McKinstry RC, Mukherjee P, et al. **Evaluating pediatric brain tumor cellularity with diffusion-tensor imaging.** *AJR Am J Roentgenol* 2001; 177:449–54
9. Guo AC, Cummings TJ, Dash RC, et al. **Lymphomas and high-grade astrocytomas: comparison of water diffusibility and histologic characteristics.** *Radiology* 2002;224:177–83
10. Tien RD, Felsberg GJ, Friedman H, et al. **MR imaging of high-grade cerebral gliomas: value of diffusion-weighted echoplanar pulse sequences.** *AJR Am J Roentgenol* 1994;162:671–77
11. Kono K, Inoue Y, Nakayama K, et al. **The role of diffusion-weighted imaging in patients with brain tumors.** *AJNR Am J Neuroradiol* 2001;22:1081–88
12. Castillo M, Smith JK, Kwock L, et al. **Apparent diffusion coefficients in the evaluation of high-grade cerebral gliomas.** *AJNR Am J Neuroradiol* 2001;22: 60–64
13. Filippi CG, Edgar MA, Ulug AM, et al. **Appearance of meningiomas on diffusion-weighted images: correlating diffusion constants with histopathologic findings.** *AJNR Am J Neuroradiol* 2001;22:65–72
14. Bulakbasi N, Guvenc I, Onguru O, et al. **The added value of the apparent diffusion coefficient calculation to magnetic resonance imaging in the differentiation and grading of malignant brain tumors.** *J Comput Assist Tomogr* 2004; 28:735–46
15. Yamasaki F, Kurisu K, Satoh K, et al. **Apparent diffusion coefficient of human brain tumors at MR imaging.** *Radiology* 2005;235:985–91
16. Calvar JA, Meli FJ, Romero C, et al. **Characterization of brain tumors by MRS, DWI and Ki-67 labeling index.** *J Neurooncol* 2005;72:273–80
17. Kotsenas AL, Roth TC, Manness WK, et al. **Abnormal diffusion-weighted MRI in medulloblastoma: does it reflect small cell histology?** *Pediatr Radiol* 1999; 29:524–26
18. Grant PE, Matsuda KM. **Application of new MR techniques in pediatric patients.** *Magn Reson Imaging Clin N Am* 2003;11:493–522
19. Camacho DLA, Smith JK, Castillo M. **Differentiation of toxoplasmosis and lymphoma in AIDS patients by using apparent diffusion coefficients.** *AJNR Am J Neuroradiol* 2003;24:633–37
20. Pauleit D, Langen KJ, Floeth F, et al. **Can the apparent diffusion coefficient be used as a noninvasive parameter to distinguish tumor tissue from peritumoral tissue in cerebral gliomas?** *J Magn Reson Imaging* 2004;20:758–64
21. Tzika AA, Zarifi MK, Goumnerova L, et al. **Neuroimaging in pediatric brain tumors: Gd-DTPA-enhanced, hemodynamic, and diffusion MR imaging compared with MR spectroscopic imaging.** *AJNR Am J Neuroradiol* 2002;23: 322–33
22. Mardor Y, Roth Y, Ochershvilli A, et al. **Pretreatment prediction of brain tumors' response to radiation therapy using high b-value diffusion-weighted MRI.** *Neoplasia* 2004;6:136–42
23. Hein PA, Eskey CJ, Dunn JF, et al. **Diffusion-weighted imaging in the follow-up of treated high-grade gliomas: tumor recurrence versus radiation injury.** *AJNR Am J Neuroradiol* 2004;25:201–09
24. Asao C, Korogi Y, Kitajima M, et al. **Diffusion-weighted imaging of radiation-induced brain injury for differentiation from tumor recurrence.** *AJNR Am J Neuroradiol* 2005;26:1455–60
25. Morriss MC, Zimmerman RA, Bilaniuk LT, et al. **Changes in brain water diffusion during childhood.** *Neuroradiology* 1999;41:929–34
26. Sener RN. **Diffusion MRI apparent diffusion coefficient (ADC) values in the normal brain and a classification of brain disorders based on ADC values.** *Comput Med Imaging Graph* 2001;25:299–326
27. Lovblad KO, Schneider J, Ruoss K, et al. **Isotropic apparent diffusion coefficient mapping of postnatal cerebral development.** *Neuroradiology* 2003;45: 400–03
28. Ellison D. **Classifying the medulloblastoma: insights from morphology and molecular genetics.** *Neuropathol Appl Neurobiol* 2002;28:257–82
29. Kleihues P, Louis DN, Scheithauer BW, et al. **The WHO classification of tumors of the nervous system.** *J Neuropathol Exp Neurol* 2002;61:215–25
30. Cheng YC, Lirng JF, Chang FC, et al. **Neuroradiological findings in atypical teratoid/rhabdoid tumor of the central nervous system.** *Acta Radiol* 2005;46: 89–96
31. Perry A. **Pathology of low-grade gliomas: an update of emerging concepts.** *Neuro-oncol* 2003;5:168–78
32. Moreno-Torres A, Martinez-Perez I, Baquero M, et al. **Taurine detection by proton magnetic resonance spectroscopy in medulloblastoma: contribution to noninvasive differential diagnosis with cerebellar astrocytoma.** *Neurosurgery* 2004;55:824–29
33. Quadery FA, Okamoto K. **Diffusion-weighted MRI of haemangioblastomas and other cerebellar tumors.** *Neuroradiology* 2003;45:212–19